IEEE Access
Multidisciplinary | Rapid Review | Open Access Journal

Received 24 February 2024, accepted 8 March 2024, date of publication 19 March 2024, date of current version 5 April 2024.

Digital Object Identifier 10.1109/ACCESS.2024.3379299

RESEARCH ARTICLE

Enhanced Satellite Synchronization Using Type-2 Asymmetric Fuzzy Brain Emotional Learning Control

NGUYEN HUU HUNG AND TIEN-LOC LE, (Member, IEEE)
Faculty of Postgraduate Studies, Lac Hong University, Bien Hoa, Dong Nai 810000, Vietnam
Faculty of Mechatronics and Electronics, Lac Hong University, Bien Hoa, Dong Nai 30019, Vietnam

Corresponding author: Tien-Loc Le (tienloc@lhu.edu.vn)

This work was supported by Lac Hong University, Bien Hoa, Dong Nai, Vietnam.

ABSTRACT This paper presents a novel approach for integrating synchronization techniques into chaotic satellite systems using type-2 fuzzy brain emotional learning control and asymmetric membership function. The proposed methodology aims to enhance the cognitive control capabilities of satellite systems, ensuring better adaptability and performance in dynamic and uncertain environments. The type-2 fuzzy brain emotional learning control system is designed to incorporate emotional learning mechanisms, enabling the satellite systems to make intelligent decisions and adapt their control strategies based on past experiences. By combining this emotional learning aspect with the asymmetric membership function, the control system gains the ability to handle uncertainties and imprecision in the system's inputs effectively. Furthermore, integrating self-organizing algorithms facilitates the automatic organization and adaptation of the control network structure, ensuring optimal system performance and scalability. To evaluate the effectiveness of the proposed approach, extensive simulations were conducted using representative scenarios of chaotic satellite systems. The results demonstrate the superiority of the type-2 fuzzy brain emotional learning control and asymmetric membership function integration, as it outperforms traditional control approaches regarding synchronization accuracy and robustness.

INDEX TERMS Brain emotional learning control, type-2 fuzzy system, self-organizing algorithm, chaotic satellite system, asymmetric membership function.

I. INTRODUCTION

In recent years, the increasing demand for more sophisticated and robust control techniques in satellite systems has driven extensive research toward exploring innovative approaches that can adapt to dynamic and uncertain environments [1], [2], [3], [4]. Chaotic satellite systems, characterized by their complex and nonlinear behavior, present unique challenges in maintaining synchronization and stability [5]. In recent years, a slew of methodologies and techniques has been proposed in the literature to achieve synchronization in a chaotic satellite system, encompassing fuzzy control [6], [7], [8], robust nonlinear control [1], [9], neural network control [9], [10], and sliding mode control [11], [12], [13]. Nevertheless, a significant portion of these methods remains intricate, leaving ample room for enhancement in terms of synchronization performance. To address these challenges, this paper proposes a novel cognitive control framework that integrates synchronization techniques into chaotic satellite systems using Type-2 Fuzzy Brain Emotional Learning Control (BELC) and Asymmetric Membership Function (AMF). Furthermore, the proposed approach leverages self-organizing algorithms to autonomously structure the control network, enhancing its adaptability and performance.

Over the last few years, BELC has found extensive application across a range of disciplines [14], [15], [16], [17], [18]. The amygdala network and the orbitofrontal cortex network (OCN) are both critical components of the BELC network, they serve separate functions and are interconnected at the final output. The fundamental difference in structure is

The associate editor coordinating the review of this manuscript and approving it for publication was Zhiguang Feng.

that, unlike the amygdala network, the orbitofrontal cortex network (OCN) does not have a firing space. This absence grants the OCN the ability to quickly respond to changes in input and makes the output calculation process faster. While the amygdala establishes emotional associations and is represented by an emotional neural network, the orbitofrontal cortex integrates sensory information and is described by a sensory neural network. The core element of the proposed approach is the type-2 fuzzy BELC system, which introduces emotional learning mechanisms inspired by the human brain's adaptive decision-making processes [19]. This aspect enables the systems to learn from past experiences and emotional responses, empowering them with the ability to make intelligent and context-aware decisions in real time [20]. Additionally, the incorporation of the AMF further enhances the control system's capabilities, enabling it to handle uncertainties, imprecision, and vagueness in the system's inputs, which are common in chaotic satellite systems. Conventional practice often employs symmetric and fixed membership functions in order to streamline the design of BELC or fuzzy systems. However, research outlined in [21] suggests that the use of symmetric MF may have a detrimental impact on system accuracy. To address this concern, Pan et al. introduced the asymmetric membership function in [22]. Recently, some notable studies have used asymmetric membership functions in their design network to improve the system performance, examples of which can be found in [23], [24], [25], [26], and [27]. In 2019, Zhao et al. presented a self-organizing interval type-2 fuzzy neural network structure with AMF for nonlinear system identification, validated through ethylene cracking furnace yield soft-sensing models [23]. In 2021, Lin et al. proposed an AMF based wavelet Petri fuzzy neural network controller for voltage stabilization in microgrid power control [25]. In previous studies, many researchers have demonstrated that type-2 fuzzy logic systems are more effective in handling uncertainty compared to normal type-1 fuzzy logic systems [28], [29], [30], [31]. This study applies a type-2 fuzzy system to asymmetric membership functions and introduces a type-2 Adaptive Membership Function (T2AMF), typically composed of two Gaussian MFs as the upper MF and two Gaussian MFs as the lower MF. This design allows it to accommodate membership functions with uncertain means and widths. This, in turn, enhances its learning capability and flexibility, as reported in [23].

The integration of synchronization techniques into the control framework is of utmost importance in maintaining the coherence and stability of satellite systems operating in chaotic conditions [32]. Synchronization ensures that all the interconnected satellites in a network behave in a coordinated manner, enabling them to achieve desired mission objectives efficiently [33]. Synchronization techniques are important in chaotic satellite systems for several reasons: communication reliability, coordination and control, security, resilience to interference and noise, distributed computing. Recent noteworthy studies on satellite systems synchronization are referenced in [8], [9], [10], [34], and [35]. In 2022, Alsaade et al. proposed a fixed-time adaptive controllers for chaotic attitude synchronization and anti-synchronization of master-slave satellites [35]. In 2023, Silahtar et al. provided two controllers, the fuzzy sliding mode controller and a new intuitionistic fuzzy sliding mode controller, for rendezvous and docking tasks of nonidentical cubic satellites [8]. The proposed approach aims to achieve synchronization while preserving the system's robustness and adaptability under varying operational conditions. Moreover, the introduction of self-organizing algorithms in the proposed framework is motivated by the need for an autonomous and scalable control network. Self-organizing algorithms facilitate the automatic organization and adaptation of the control system, allowing it to reconfigure its structure based on the changing dynamics of the satellite system. This characteristic ensures that the control network remains optimal and efficient, even when the system encounters uncertainties or new challenges.

To evaluate the effectiveness of the proposed approach, comprehensive simulations were conducted using representative scenarios of chaotic satellite systems. The simulation results demonstrate the superiority of the type-2 fuzzy BELC and AMF integration, as it outperforms traditional control approaches in terms of synchronization accuracy and robustness. Furthermore, the self-organizing algorithms showcase their ability to dynamically structure and optimize the control network, thereby improving the overall system performance. The main contribution of this study is the design of a novel approach for integrating synchronization techniques into chaotic satellite systems through the combination of Type-2 Fuzzy BELC, AMF, and Self-Organizing algorithms (ST2ABELC). The proposed cognitive control framework demonstrates promising results and holds great potential for revolutionizing the control of complex satellite systems in real-world applications. The adaptability, robustness, and synchronization capabilities of the proposed approach make it a compelling solution for addressing the challenges posed by chaotic satellite systems and enhancing their overall performance in various dynamic and uncertain scenarios.

II. PROBLEM FORMULATION

Let's consider the chaotic satellite systems, termed the master and slave systems, as described in [3]:

$$\begin{aligned}
\dot{a}_1(t) &= \lambda_1 a_2(t) a_3(t) - \frac{1.2}{T_1} a_1(t) + \frac{\sqrt{6}}{2T_1} a_3(t) \\
\dot{a}_2(t) &= \lambda_2 a_1(t) a_3(t) + \frac{0.35}{T_2} x_2(t) \\
\dot{a}_3(t) &= \lambda_3 a_1(t) a_2(t) - \frac{\sqrt{6}}{T_3} a_1(t) - \frac{0.4}{T_3} a_3(t)
\end{aligned} \tag{1}$$

and

$$\begin{aligned}
\dot{b}_1(t) &= \lambda_1 b_2(t) b_3(t) - \frac{1.2}{T_1} b_1(t) + \frac{\sqrt{6}}{2T_1} b_3(t) + \varepsilon_1(t) \\
&\quad + \Delta f(b_1) + \upsilon_1(t) \\
\dot{b}_2(t) &= \lambda_2 b_1(t) b_3(t) + \frac{0.35}{T_2} b_2(t) + \varepsilon_2(t) + \Delta f(b_2) + \upsilon_2(t)
\end{aligned}$$

$$\dot{b}_3(t) = \lambda_3 b_1(t) b_2(t) - \frac{\sqrt{6}}{T_3} b_1(t) - \frac{0.4}{T_3} b_3(t) + \varepsilon_3(t) + \Delta f(b_3) + \upsilon_3(t) \quad (2)$$

where $\boldsymbol{a}(t) = [a_1(t), a_2(t), a_3(t)]$ and $\boldsymbol{b}(t) = [b_1(t), b_2(t), b_3(t)]$ represent the chaotic positions of the master and slave systems; T_1, T_2, T_3 represent the primary inertia coefficients; $\lambda_1 = \frac{T_2 - T_3}{T_1}$, $\lambda_2 = \frac{T_3 - T_1}{T_2}$, $\lambda_3 = \frac{T_1 - T_2}{T_3}$ denote the chaotic coefficients; $\boldsymbol{\varepsilon}(t) = [\varepsilon_1(t), \varepsilon_2(t), \varepsilon_3(t)]$ and $\Delta \boldsymbol{f}(b) = [\Delta(b_1), \Delta b_2(t), \Delta b_3(t)]$ represent the external disturbances and system uncertainties, respectively; $\boldsymbol{\upsilon}(t) = [\upsilon_1(t), \upsilon_2(t), \upsilon_3(t)]$ correspond to the input control torques signal.

Rewrite (1) and (2) in vector form as follows:

$$\dot{\boldsymbol{a}}(t) = \boldsymbol{H}(a(t)) \quad (3)$$

$$\dot{\boldsymbol{b}}(t) = \boldsymbol{H}(b(t)) + \boldsymbol{\varepsilon}(t) + \Delta \boldsymbol{f}(b(t)) + \boldsymbol{\upsilon}(t) \quad (4)$$

The vector synchronization errors between the master and slave chaotic systems are denote as $\boldsymbol{e}(t) = [e_1(t), e_2(t), e_3(t)]$, which can be expressed as:

$$\begin{aligned} e_1(t) &= b_1(t) - a_1(t) \\ e_2(t) &= b_2(t) - a_2(t) \\ e_3(t) &= b_3(t) - a_3(t) \end{aligned} \quad (5)$$

Consequently, the error dynamics can be represented as:

$$\begin{aligned} \dot{e}_1(t) &= \lambda_1 \left(b_2(t) b_3(t) - a_2(t) a_3(t)\right) - \frac{1.2}{T_1} e_1 \\ &\quad + \frac{\sqrt{6}}{2T_1} e_3 + \varepsilon_1(t) + \Delta f(b_1) + \upsilon_1(t) \\ \dot{e}_2(t) &= \lambda_2 \left(b_1(t) b_3(t) - a_1(t) a_3(t)\right) + \frac{0.35}{T_2} e_2(t) + \varepsilon_2(t) \\ &\quad + \Delta f(b_2) + \upsilon_2(t) \\ \dot{e}_3(t) &= \lambda_3 \left(b_1(t) b_2(t) - a_1(t) a_2(t)\right) - \frac{\sqrt{6}}{T_3} e_1(t) \\ &\quad - \frac{0.4}{I_z} e_3(t) + \varepsilon_3(t) + \Delta f(b_3) + \upsilon_3(t) \end{aligned} \quad (6)$$

Vector error Dynamics can be obtain as follows:

$$\dot{\boldsymbol{e}}(t) = \boldsymbol{H}\boldsymbol{e}(t) + \boldsymbol{f}(t) + \boldsymbol{\varepsilon}(t) + \Delta \boldsymbol{f}(b(t)) + \boldsymbol{\upsilon}(t) \quad (7)$$

where

$$\boldsymbol{H} = \begin{bmatrix} \frac{-1.2}{T_1} & 0 & \frac{\sqrt{6}}{2T_1} \\ 0 & \frac{0.35}{T_2} & 0 \\ \frac{-\sqrt{6}}{2T_3} & 0 & \frac{-0.4}{T_3} \end{bmatrix};$$

$$\boldsymbol{f}(t) = \begin{bmatrix} \lambda_1 \left(b_2(t) b_3(t) - a_2(t) a_3(t)\right) \\ \lambda_2 \left(b_1(t) b_3(t) - a_1(t) a_3(t)\right) \\ \lambda_3 \left(b_1(t) b_2(t) - a_1(t) a_2(t)\right) \end{bmatrix}$$

Considering (7), the design of the ideal controller becomes feasible:

$$\boldsymbol{u}^*(t) = -\boldsymbol{H}\boldsymbol{e}(t) - \boldsymbol{f}(t) - \boldsymbol{\varepsilon}(t) - \Delta \boldsymbol{f}(b(t)) - \dot{\boldsymbol{e}}(t) \quad (8)$$

Nonetheless, it is imperative to recognize that the precise knowledge of external disturbances and system uncertainties in equation (8) remains unattainable. Consequently, in this investigation, we present the ST2ABELC controller, devised to mimic the ideal controller and accomplish the synchronization of the master and slave chaotic satellite systems.

III. STRUCTURE OF ST2ABELC CONTROLLER

Figure 1 illustrates the schematic synchronized diagram of the chaotic satellite systems synchronization, termed ST2ABELC, designed for chaotic satellite systems synchronization. Figure 2 depicts the architecture of ST2ABELC, comprising the amygdala network and the orbitofrontal cortex network.

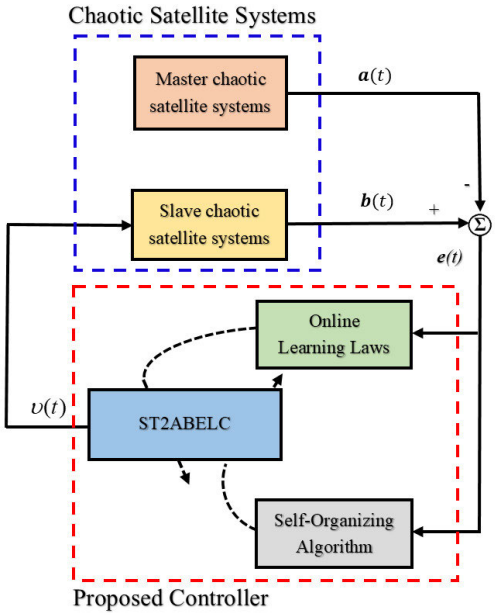

FIGURE 1. Schematic synchronize diagram of the chaotic satellite systems synchronization.

The amygdala system's rule for a sensory neural network can be expressed as follows:

$$\begin{aligned} &IF\ I_1 \text{ is } \varphi_{1j} \text{ and } \ldots \text{ and } I_i \text{ is } \varphi_{ij} \text{ and } \ldots \text{ and } I_{n_i} \text{ is } \varphi_{n_i j} \\ &THEN a_k = \theta_{jk} \text{ for } i = 1, \ldots, n_i;\ j = 1, \ldots, n_j; \\ &\qquad k = 1, \ldots, n_k \end{aligned} \quad (9)$$

where n_i and n_k respectively are the number of inputs and the number of outputs; n_j is the number of membership function in each inputs. $\varphi_{ij} = \left[\underline{\varphi}_{ij} \overline{\varphi}_{ij}\right]$ and $\theta_{jk} = \left[\underline{\theta}_{jk} \overline{\theta}_{jk}\right]$ stand for the range values defining the membership grades and the amygdala weights, respectively.

The orbitofrontal system's rule for an emotional neural network can be expressed as follows:

$$\begin{aligned} &\text{IF } I_1 \text{ is } \delta_{1j} \text{ and } \ldots \text{ and } I_i \text{ is } \delta_{ij} \text{ and } \ldots \text{ and } I_{n_i} \text{ is } \delta_{n_i j} \\ &\text{THEN } o_k = \upsilon_{ijk} \end{aligned} \quad (10)$$

where $\delta_{ij} = \left[\underline{\delta}_{ij} \overline{\delta}_{ij}\right]$ and $\upsilon_{ijk} = \left[\underline{\upsilon}_{ijk} \overline{\upsilon}_{ijk}\right]$ stand for the range values defining the membership grades and the amygdala weights, respectively.

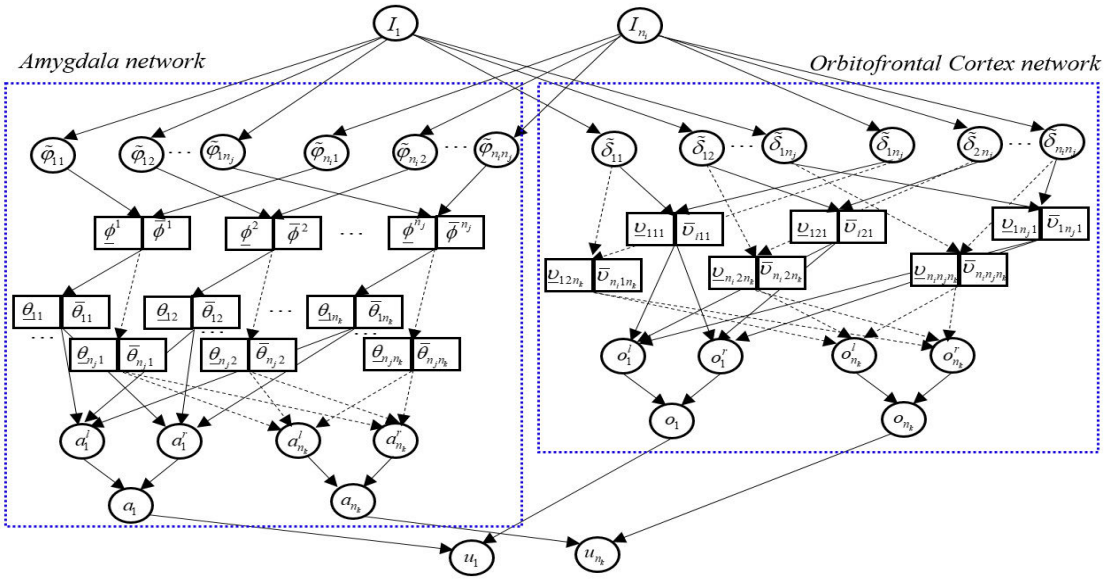

FIGURE 2. Structure of the proposed ST2ABELC network.

Then, the k^{th} output in ST2ABELC is computed as follows:

$$u^k_{ST2ABELC} = a_k - o_k \quad \text{for } k = 1,\ 2,\ \ldots,\ n_k \tag{11}$$

where a_k and o_k are the output of the amygdala network and the orbitofrontal cortex network, respectively.

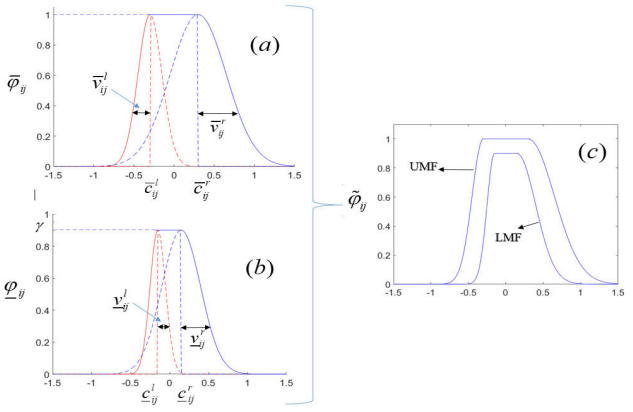

FIGURE 3. Type-2 Asymmetric GMFs. (a) upper membership function; (b) lower membership function; (c) combined T2AMF.

A. THE AMYGDALA NETWORK

The amygdala network exhibits a unique configuration as an IT2FNN, encompassing five spaces. The process of signal propagation and the fundamental operations within each of these spaces are elucidated below.

1) THE INPUT SPACE

Nodes within this space are denoted by $I = [I_1, I_2, \ldots I_i, \ldots I_{n_i}]^T \in \Re^{n_i}$, where I_i stand for the i^{th} input, and n_i represent the count of input signals. This space is dedicated solely to reception, without any computational processes; consequently, all nodes will be seamlessly passed on to the subsequent space.

2) THE MEMBERSHIP FUNCTION SPACE

This space performs calculations of membership grades based on the input variables I_i, utilizing the type-2 asymmetric Gaussian membership function (T2AGMF). Shown in Figure 3, the T2AGMF exhibits the inherent uncertainties in its standard deviation denoted as $\tilde{v}^l_{ij} \in \left[\underline{v}^l_{ij}, \overline{v}^l_{ij}\right]$ and $\tilde{v}^r_{ij} \in \left[\underline{v}^r_{ij}, \overline{v}^r_{ij}\right]$. As a result, the outputs from this space yield uncertain membership grades $\tilde{\varphi}_{ij} \in \left[\underline{\varphi}_{ij}, \overline{\varphi}_{ij}\right]$, which are defined as follows:

$$\overline{\varphi}_{ij} = \begin{cases} \exp\left\{\dfrac{-\left(I_i - \overline{c}^l_{ij}\right)^2}{2\left(\overline{v}^l_{ij}\right)^2}\right\}, & I_i \le \overline{c}^l_{ij} \\ 1, & \overline{c}^l_{ij} \le I_i \le \overline{c}^r_{ij} \\ \exp\left\{\dfrac{-\left(I_i - \overline{c}^r_{ij}\right)^2}{2\left(\overline{v}^r_{ij}\right)^2}\right\}, & \overline{c}^r_{ij} \le I_i \end{cases} \tag{12}$$

$$\underline{\varphi}_{ij} = \begin{cases} \gamma^* \exp\left\{\dfrac{-\left(I_i - \underline{c}^l_{ij}\right)^2}{2\left(\underline{v}^l_{ij}\right)^2}\right\}, & I_i \le \underline{c}^l_{ij} \\ \gamma, & \underline{c}^l_{ij} \le I_i \le \underline{c}^r_{ij} \\ \gamma^* \exp\left\{\dfrac{-\left(I_i - \underline{c}^r_{ij}\right)^2}{2\left(\underline{v}^r_{ij}\right)^2}\right\}, & \underline{c}^r_{ij} \le I_i \end{cases} \tag{13}$$

To prevent the emergence of inappropriate membership functions, it is essential to incorporate the following constraints

$$\begin{cases} \overline{c}_{ij}^{l} \le \underline{c}_{ij}^{l} \le \underline{c}_{ij}^{r} \le \overline{c}_{ij}^{r} \\ \underline{v}_{ij}^{l} \le \overline{v}_{ij}^{l} \le \underline{v}_{ij}^{r} \le \overline{v}_{ij}^{r} \\ 0.5 \le \gamma \le 1 \end{cases} \tag{14}$$

where $\overline{\varphi}_{ij}$ and $\underline{\varphi}_{ij}$ represent the upper and lower bounds of the membership function, respectively. Additionally, $\overline{c}_{ij}^{l}$ and $\overline{c}_{ij}^{r}$ denote the means of the two upper Gaussian membership functions, while $\overline{v}_{ij}^{l}$ and $\overline{v}_{ij}^{r}$ represent their variances. Furthermore, $\underline{c}^{l}{}_{ij}$ and $\underline{c}^{r}{}_{ij}$ signify the means of the two lower Gaussian membership functions, and $\underline{v}^{l}{}_{ij}$ and $\underline{v}^{r}{}_{ij}$ indicate their variances.

3) THE FIRING SPACE

In this space, the fuzzy firing operation is conducted, leveraging the membership grades derived from the preceding space. The output corresponding to the j-th rule within this domain can be defined as:

$$\overline{\phi}^{j} = \prod_{i=1}^{n_i} \overline{\varphi}_{ij} \tag{15}$$

$$\underline{\phi}^{j} = \prod_{i=1}^{n_i} \underline{\varphi}_{ij} \tag{16}$$

4) THE WEIGHT MEMORY SPACE

Within this space, the fuzzy rule is executed using the weights of the amygdala network. Due to the interval nature of the firing domain, the weights are also represented as interval values. The weight associated with the i-th rule and k-th output of the amygdala network can be expressed as:

$$\tilde{\theta}_{jk} = \left[\underline{\theta}_{jk} \overline{\theta}_{jk}\right] \tag{17}$$

5) THE AMYGDALA OUTPUT SPACE

The defuzzification process in the premise parts of fuzzy rules is executed using product operations within this space. The amygdala network's output in this space is determined through a combination of the firing space output and the output weight space.

$$a_k = \frac{a_k^l + a_k^r}{2} = \frac{1}{2}\frac{\sum_{j=1}^{n_j} \underline{\phi}^{j} \underline{\theta}_{jk}}{\sum_{j=1}^{n_j} \underline{\phi}^{j}} + \frac{1}{2}\frac{\sum_{j=1}^{n_j} \overline{\phi}^{j} \overline{\theta}_{jk}}{\sum_{j=1}^{n_j} \overline{\phi}^{j}} \tag{18}$$

B. THE ORBITOFRONTAL CORTEX NETWORK

This network has four spaces. The process of signal propagation and the fundamental operations within each of these spaces are elucidated below.

1) THE INPUT SPACE

This space consists of nodes that share the same vector input $I = \left[I_1, I_2, \ldots I_i, \ldots I_{n_i}\right]^T \in \Re^{n_i}$ as the amygdala network's input. In this space, there are no computational processes, and all nodes are seamlessly passed on to the subsequent space.

2) THE MEMBERSHIP FUNCTION SPACE

In this space, membership grades are computed based on I_i. For efficient and fast computation, the T2GMFs are utilized as follows:

$$\overline{\delta}_{ij} = \exp\left\{-\frac{1}{2}\left(\frac{I_i - \kappa_{ik}}{\overline{\tau}_{ik}}\right)^2\right\} \tag{19}$$

$$\underline{\delta}_{ij} = \exp\left\{-\frac{1}{2}\left(\frac{I_i - \kappa_{ij}}{\underline{\tau}_{ij}}\right)^2\right\} \tag{20}$$

3) THE WEIGHT MEMORY SPACE

Within this space, the fuzzy rule is executed using the connecting weights. The weight associated with the i-th rule, j-th layer, and k-th output can be expressed as:

$$\tilde{\upsilon}_{ijk} = \left[\underline{\upsilon}_{ijk} \overline{\upsilon}_{ijk}\right] \tag{21}$$

4) THE ORBITOFRONTAL OUTPUT SPACE

This arena executes the defuzzification process by employing the center of gravity algorithm. The orbitofrontal network's output in this space is determined through a combination of the membership grades and the weight memory space.

$$o_k = \frac{o_k^l + o_k^r}{2} = \frac{1}{2}\frac{\sum_{j=1}^{n_j}\sum_{i=1}^{n_i} \underline{\delta}_{ij}\underline{\upsilon}_{ijk}}{\sum_{j=1}^{n_j}\sum_{i=1}^{n_i} \underline{\delta}_{ij}} + \frac{1}{2}\frac{\sum_{j=1}^{n_j}\sum_{i=1}^{n_i} \overline{\delta}_{ij}\overline{\upsilon}_{ijk}}{\sum_{j=1}^{n_j}\sum_{i=1}^{n_i} \overline{\delta}_{ij}} \tag{22}$$

C. THE PARAMETER ADAPTATION DESIGN FOR ST2ABELC CONTROLLER

First, the energy function is defined as: $E = \frac{1}{2}(e_k(t))^2$, where e_k can be substituted with e_1, e_2, and e_3 in (5). Then, employing the gradient descent technique in conjunction with the chain rule, the online adjustment regulations for the parameters of ST2ABELC are given as follows:

1) THE PARAMETER ADAPTATION DESIGN FOR AMYGDALA NETWORK

$$\begin{aligned} \underline{\theta}_{jk}(t+1) &= \underline{\theta}_{jk}(t) - \hat{\eta}_{\theta}\frac{\partial E(t)}{\partial \underline{\theta}_{jk}} \\ &= \underline{\theta}_{jk}(t) - \eta_{\theta}\frac{\partial E(t)}{\partial \hat{u}_{ST2ABELC}^{k}}\frac{\partial \hat{u}_{ST2ABELC}^{k}}{\partial a_k}\frac{\partial a_k}{\partial a_k^l}\frac{\partial a_k^l}{\partial \underline{\theta}_{jk}} \\ &= \underline{\theta}_{jk}(t) + \eta_{\theta}\frac{1}{2}e_k(t)\frac{\underline{\phi}^{j}}{\sum_{j=1}^{n_j}\underline{\phi}^{j}} \end{aligned} \tag{23}$$

$$\begin{aligned} \overline{\theta}_{jk}(t+1) &= \overline{\theta}_{jk}(t) - \eta_{\theta}\frac{\partial E(t)}{\partial \overline{\theta}_{jk}} \\ &= \overline{\theta}_{jk}(t) - \eta_{\theta}\frac{\partial E(t)}{\partial \hat{u}_{ST2ABELC}^{k}}\frac{\partial \hat{u}_{ST2ABELC}^{k}}{\partial a_k}\frac{\partial a_k}{\partial a_k^r}\frac{\partial a_k^r}{\partial \overline{\theta}_{jk}} \\ &= \overline{\theta}_{jk}(t) + \eta_{\theta}\frac{1}{2}e_k(t)\frac{\overline{\phi}^{j}}{\sum_{j=1}^{n_j}\overline{\phi}^{j}} \end{aligned} \tag{24}$$

$$\begin{aligned}\underline{c}^{l}_{ij}(t+1) &= \underline{c}^{l}_{ij}(t) - \eta_c \frac{\partial E(t)}{\partial \underline{c}^{l}_{ij}} \\ &= \underline{c}^{l}_{ij}(t) - \eta_c \\ &\quad \times \left(\frac{\partial E(t)}{\partial \hat{u}_{ST2ABELC}} \frac{\partial \hat{u}_{ST2ABELC}}{\partial a^{l}_{k}} \frac{\partial a^{l}_{k}}{\partial \underline{\phi}^{j}} \frac{\partial \underline{\phi}^{j}}{\partial \underline{\varphi}_{ij}} \frac{\partial \underline{\varphi}_{ij}}{\partial \underline{c}^{l}_{ij}} \right) \\ &= \underline{c}^{l}_{ij}(t) - \frac{1}{2}\eta_c e_k(t) \left(\frac{\underline{\theta}_{jk} - a^{l}_{k}}{\sum_{j=1}^{n_j} \underline{\phi}^{j}} \right) \left(\frac{\underline{\phi}^{j}}{\underline{\varphi}_{ij}} \right) \frac{\partial \underline{\varphi}_{ij}}{\partial \underline{c}^{l}_{ij}} \end{aligned} \tag{25}$$

$$\begin{aligned}\underline{c}^{r}_{ij}(t+1) &= \underline{c}^{r}_{ij}(t) - \eta_c \frac{\partial E(t)}{\partial \underline{c}^{r}_{ij}} \\ &= \underline{c}^{r}_{ij}(t) - \eta_c \\ &\quad \times \left(\frac{\partial E(t)}{\partial \hat{u}_{ST2ABELC}} \frac{\partial \hat{u}_{ST2ABELC}}{\partial a^{l}_{k}} \frac{\partial a^{l}_{k}}{\partial \underline{\phi}^{j}} \frac{\partial \underline{\phi}^{j}}{\partial \underline{\varphi}_{ij}} \frac{\partial \underline{\varphi}_{ij}}{\partial \underline{c}^{r}_{ij}} \right) \\ &= \underline{c}^{r}_{ij}(t) - \frac{1}{2}\eta_c e_k(t) \left(\frac{\underline{\theta}_{jk} - a^{l}_{k}}{\sum_{j=1}^{n_j} \underline{\phi}^{j}} \right) \left(\frac{\underline{\phi}^{j}}{\underline{\varphi}_{ij}} \right) \frac{\partial \underline{\varphi}_{ij}}{\partial \underline{c}^{r}_{ij}} \end{aligned} \tag{26}$$

$$\begin{aligned}\underline{v}^{l}_{ij}(t+1) &= \underline{v}^{l}_{ij}(t) - \eta_v \frac{\partial E(t)}{\partial \underline{v}^{l}_{ij}} \\ &= \underline{v}^{l}_{ij}(t) - \eta_v \\ &\quad \times \left(\frac{\partial E(t)}{\partial \hat{u}_{ST2ABELC}} \frac{\partial \hat{u}_{ST2ABELC}}{\partial a^{l}_{k}} \frac{\partial a^{l}_{k}}{\partial \underline{\phi}^{j}} \frac{\partial \underline{\phi}^{j}}{\partial \underline{\varphi}_{ij}} \frac{\partial \underline{\varphi}_{ij}}{\partial \underline{v}^{l}_{ij}} \right) \\ &= \underline{v}^{l}_{ij}(t) - \frac{1}{2}\eta_v e_k(t) \left(\frac{\underline{\theta}_{jk} - a^{l}_{k}}{\sum_{j=1}^{n_j} \underline{\phi}^{j}} \right) \left(\frac{\underline{\phi}^{j}}{\underline{\varphi}_{ij}} \right) \frac{\partial \underline{\varphi}_{ij}}{\partial \underline{v}^{l}_{ij}} \end{aligned} \tag{27}$$

$$\begin{aligned}\underline{v}^{r}_{ij}(t+1) &= \underline{v}^{r}_{ij}(t) - \eta_v \frac{\partial E(t)}{\partial \underline{v}^{r}_{ij}} \\ &= \underline{v}^{r}_{ij}(t) - \eta_v \\ &\quad \times \left(\frac{\partial E(t)}{\partial \hat{u}_{ST2ABELC}} \frac{\partial \hat{u}_{ST2ABELC}}{\partial a^{l}_{k}} \frac{\partial a^{l}_{k}}{\partial \underline{\phi}^{j}} \frac{\partial \underline{\phi}^{j}}{\partial \underline{\varphi}_{ij}} \frac{\partial \underline{\varphi}_{ij}}{\partial \underline{v}^{r}_{ij}} \right) \\ &= \underline{v}^{r}_{ij}(t) - \frac{1}{2}\eta_v e_k(t) \left(\frac{\underline{\theta}_{jk} - a^{l}_{k}}{\sum_{j=1}^{n_j} \underline{\phi}^{j}} \right) \left(\frac{\underline{\phi}^{j}}{\underline{\varphi}_{ij}} \right) \frac{\partial \underline{\varphi}_{ij}}{\partial \underline{v}^{r}_{ij}} \end{aligned} \tag{28}$$

$$\begin{aligned}\overline{c}^{l}_{ij}(t+1) &= \overline{c}^{l}_{ij}(t) - \eta_c \frac{\partial E(t)}{\partial \overline{c}^{l}_{ij}} \\ &= \overline{c}^{l}_{ij}(t) - \eta_c \\ &\quad \times \left(\frac{\partial E(t)}{\partial \hat{u}_{ST2ABELC}} \frac{\partial \hat{u}_{ST2ABELC}}{\partial a^{r}_{k}} \frac{\partial a^{r}_{k}}{\partial \overline{\phi}^{j}} \frac{\partial \overline{\phi}^{j}}{\partial \overline{\varphi}_{ij}} \frac{\partial \overline{\varphi}_{ij}}{\partial \overline{c}^{l}_{ij}} \right) \\ &= \overline{c}^{l}_{ij}(t) - \frac{1}{2}\eta_c e_k(t) \left(\frac{\overline{\theta}_{jk} - a^{r}_{k}}{\sum_{j=1}^{n_j} \overline{\phi}^{j}} \right) \left(\frac{\overline{\phi}^{j}}{\overline{\varphi}_{ij}} \right) \frac{\partial \overline{\varphi}_{ij}}{\partial \overline{c}^{l}_{ij}} \end{aligned} \tag{29}$$

$$\begin{aligned}\overline{c}^{r}_{ij}(t+1) &= \overline{c}^{r}_{ij}(t) - \eta_c \frac{\partial E(t)}{\partial \overline{c}^{r}_{ij}} \\ &= \overline{c}^{r}_{ij}(t) - \eta_c \\ &\quad \left(\frac{\partial E(t)}{\partial \hat{u}_{ST2ABELC}} \frac{\partial \hat{u}_{ST2ABELC}}{\partial a^{r}_{k}} \frac{\partial a^{r}_{k}}{\partial \overline{\phi}^{j}} \frac{\partial \overline{\phi}^{j}}{\partial \overline{\varphi}_{ij}} \frac{\partial \overline{\varphi}_{ij}}{\partial \overline{c}^{r}_{ij}} \right) \\ &= \overline{c}^{r}_{ij}(t) - \frac{1}{2}\eta_c e_k(t) \left(\frac{\overline{\theta}_{jk} - a^{r}_{k}}{\sum_{j=1}^{n_j} \overline{\phi}^{j}} \right) \left(\frac{\overline{\phi}^{j}}{\overline{\varphi}_{ij}} \right) \frac{\partial \overline{\varphi}_{ij}}{\partial \overline{c}^{r}_{ij}} \end{aligned} \tag{30}$$

$$\begin{aligned}\overline{v}^{l}_{ij}(t+1) &= \overline{v}^{l}_{ij}(t) - \eta_v \frac{\partial E(t)}{\partial \overline{v}^{l}_{ij}} \\ &= \overline{v}^{l}_{ij}(t) - \eta_v \\ &\quad \left(\frac{\partial E(t)}{\partial \hat{u}_{ST2ABELC}} \frac{\partial \hat{u}_{ST2ABELC}}{\partial a^{r}_{k}} \frac{\partial a^{r}_{k}}{\partial \overline{\phi}^{j}} \frac{\partial \overline{\phi}^{j}}{\partial \overline{\varphi}_{ij}} \frac{\partial \overline{\varphi}_{ij}}{\partial \overline{v}^{l}_{ij}} \right) \\ &= \overline{v}^{l}_{ij}(t) - \frac{1}{2}\eta_v e_k(t) \left(\frac{\overline{\theta}_{jk} - a^{r}_{k}}{\sum_{j=1}^{n_j} \overline{\phi}^{j}} \right) \left(\frac{\overline{\phi}^{j}}{\overline{\varphi}_{ij}} \right) \frac{\partial \overline{\varphi}_{ij}}{\partial \overline{v}^{l}_{ij}} \end{aligned} \tag{31}$$

$$\begin{aligned}\overline{v}^{r}_{ij}(t+1) &= \overline{v}^{r}_{ij}(t) - \eta_v \frac{\partial E(t)}{\partial \overline{v}^{r}_{ij}} \\ &= \overline{v}^{r}_{ij}(t) - \eta_v \\ &\quad \times \left(\frac{\partial E(t)}{\partial \hat{u}_{ST2ABELC}} \frac{\partial \hat{u}_{ST2ABELC}}{\partial a^{r}_{k}} \frac{\partial a^{r}_{k}}{\partial \overline{\phi}^{j}} \frac{\partial \overline{\phi}^{j}}{\partial \overline{\varphi}_{ij}} \frac{\partial \overline{\varphi}_{ij}}{\partial \overline{v}^{r}_{ij}} \right) \\ &= \overline{v}^{r}_{ij}(t) - \frac{1}{2}\eta_v e_k(t) \left(\frac{\overline{\theta}_{jk} - a^{r}_{k}}{\sum_{j=1}^{n_j} \overline{\phi}^{j}} \right) \left(\frac{\overline{\phi}^{j}}{\overline{\varphi}_{ij}} \right) \\ &\quad \times \frac{\partial \overline{\varphi}_{ij}}{\partial \overline{v}^{r}_{ij}} \end{aligned} \tag{32}$$

where η_θ, η_c, η_v are the positive learning-rates. Depending on the regions of current input, the derivative terms $\frac{\partial \underline{\varphi}_{ij}}{\partial \underline{c}^{l}_{ij}}$, $\frac{\partial \underline{\varphi}_{ij}}{\partial \underline{c}^{r}_{ij}}$, $\frac{\partial \underline{\varphi}_{ij}}{\partial \underline{v}^{l}_{ij}}$, $\frac{\partial \underline{\varphi}_{ij}}{\partial \underline{v}^{r}_{ij}}$ in (25)-(28) and $\frac{\partial \overline{\varphi}_{ij}}{\partial \overline{c}^{l}_{ij}}$, $\frac{\partial \overline{\varphi}_{ij}}{\partial \overline{c}^{r}_{ij}}$, $\frac{\partial \overline{\varphi}_{ij}}{\partial \overline{v}^{l}_{ij}}$, $\frac{\partial \overline{\varphi}_{ij}}{\partial \overline{v}^{r}_{ij}}$ in (29)-(32) can be determined in Table 1 and Table 2, respectively.

TABLE 1. The cases for updating lower MFs.

Case1: $I_i \le \underline{c}_{ij}^l$	**Case 2:** $\underline{c}_{ij}^l \le I_i \le \underline{c}_{ij}^r$	**Case 3:** $\underline{c}_{ij}^r \le I$
$\frac{\partial \underline{\varphi}_{ij}}{\partial \underline{c}_{ij}^l} = \underline{\varphi}_{ij} \frac{\left(I_i - \underline{c}_{ij}^l\right)}{\left(\underline{v}_{ij}^l\right)^2}$	$\frac{\partial \underline{\varphi}_{ij}}{\partial \underline{c}_{ij}^l} = 0$	$\frac{\partial \underline{\varphi}_{ij}}{\partial \underline{c}_{ij}^l} = 0$
$\frac{\partial \underline{\varphi}_{ij}}{\partial \underline{c}_{ij}^r} = 0$	$\frac{\partial \underline{\varphi}_{ij}}{\partial \underline{c}_{ij}^r} = 0$	$\frac{\partial \underline{\varphi}_{ij}}{\partial \underline{c}_{ij}^r} = \underline{\varphi}_{ij} \frac{\left(I_i - \underline{c}_{ij}^r\right)}{\left(\underline{v}_{ij}^r\right)^2}$
$\frac{\partial \underline{\varphi}_{ij}}{\partial \underline{v}_{ij}^l} = \underline{\varphi}_{ij} \frac{\left(I_i - \underline{c}_{ij}^l\right)^2}{\left(\underline{v}_{ij}^l\right)^3}$	$\frac{\partial \underline{\varphi}_{ij}}{\partial \underline{v}_{ij}^l} = 0$	$\frac{\partial \underline{\varphi}_{ij}}{\partial \underline{v}_{ij}^l} = 0$
$\frac{\partial \underline{\varphi}_{ij}}{\partial \underline{v}_{ij}^r} = 0$	$\frac{\partial \underline{\varphi}_{ij}}{\partial \underline{v}_{ij}^r} = 0$	$\frac{\partial \underline{\varphi}_{ij}}{\partial \underline{v}_{ij}^r} = \underline{\varphi}_{ij} \frac{\left(I_i - \underline{c}_{ij}^r\right)^2}{\left(\underline{v}_{ij}^r\right)^3}$

TABLE 2. The cases for updating upper MFs.

Case1: $I_i \le \overline{c}_{ij}^l$	**Case 2:** $\overline{c}_{ij}^l \le I_i \le \overline{c}_{ij}^r$	**Case 3:** $\overline{c}_{ij}^r \le I_i$
$\frac{\partial \overline{\varphi}_{ij}}{\partial \overline{c}_{ij}^l} = \overline{\varphi}_{ij} \frac{\left(I_i - \overline{c}_{ij}^l\right)}{\left(\overline{v}_{ij}^l\right)^2}$	$\frac{\partial \overline{\varphi}_{ij}}{\partial \overline{c}_{ij}^l} = 0$	$\frac{\partial \overline{\varphi}_{ij}}{\partial \overline{c}_{ij}^l} = 0$
$\frac{\partial \overline{\varphi}_{ij}}{\partial \overline{c}_{ij}^r} = 0$	$\frac{\partial \overline{\varphi}_{ij}}{\partial \overline{c}_{ij}^r} = 0$	$\frac{\partial \overline{\varphi}_{ij}}{\partial \overline{c}_{ij}^r} = \overline{\varphi}_{ij} \frac{\left(I_i - \overline{c}_{ij}^r\right)}{\left(\overline{v}_{ij}^r\right)^2}$
$\overline{\varphi}_{ij} \frac{\left(I_i - \overline{c}_{ij}^l\right)^2}{\left(\overline{v}_{ij}^l\right)^3}$	$\frac{\partial \overline{\varphi}_{ij}}{\partial \overline{v}_{ij}^l} = 0$	$\frac{\partial \overline{\varphi}_{ij}}{\partial \overline{v}_{ij}^l} = 0$
$\frac{\partial \overline{\varphi}_{ij}}{\partial \overline{v}_{ij}^r} = 0$	$\frac{\partial \overline{\varphi}_{ij}}{\partial \overline{v}_{ij}^r} = 0$	$\frac{\partial \overline{\varphi}_{ij}}{\partial \overline{v}_{ij}^r} = \overline{\varphi}_{ij} \frac{\left(I_i - \overline{c}_{ij}^r\right)^2}{\left(\overline{v}_{ij}^r\right)^3}$

2) THE PARAMETER ADAPTATION DESIGN FOR ORBITOFRONTAL CORTEX NETWORK

$$\begin{aligned}\underline{\upsilon}_{ijk}(t+1) &= \underline{\upsilon}_{ijk}(t) - \eta_\upsilon \frac{\partial E(t)}{\partial \underline{\upsilon}_{ijk}} \\ &= \underline{\upsilon}_{ijk}(t) - \eta_\upsilon \frac{\partial E(t)}{\partial \hat{u}_{ST2ABELC}^k} \frac{\partial \hat{u}_{ST2ABELC}^k}{\partial o_k} \frac{\partial o_k}{\partial o_k^l} \\ &\quad \times \frac{\partial o_k^l}{\partial \underline{\upsilon}_{ijk}} \\ &= \underline{\upsilon}_{ijk}(t) + \eta_\upsilon \frac{1}{2} e_k(t) \frac{\underline{\delta}_{ij}}{\sum_{i=1}^{n_i} \sum_{j=1}^{n_j} \underline{\delta}_{ij}} \end{aligned} \tag{33}$$

$$\begin{aligned}\overline{\upsilon}_{ijk}(t+1) &= \overline{\upsilon}_{ijk}(t) - \eta_\upsilon \frac{\partial E(t)}{\partial \overline{\upsilon}_{ijk}} \\ &= \overline{\upsilon}_{ijk}(t) - \eta_\upsilon \frac{\partial E(t)}{\partial \hat{u}_{ST2ABELC}^k} \frac{\partial \hat{u}_{ST2ABELC}^k}{\partial o_k} \frac{\partial o_k}{\partial o_k^r} \\ &\quad \times \frac{\partial o_k^r}{\partial \overline{\upsilon}_{ijk}} \\ &= \overline{\upsilon}_{ijk}(t) + \eta_\upsilon \frac{1}{2} e_k(t) \frac{\overline{\delta}_{ij}}{\sum_{i=1}^{n_i} \sum_{j=1}^{n_j} \overline{\delta}_{ij}} \end{aligned} \tag{34}$$

$$\begin{aligned}\kappa_{ik}(t+1) &= \kappa_{ik}(t) - \eta_\upsilon \frac{\partial E(t)}{\partial \kappa_{ik}} \\ &= \kappa_{ik}(t) - \eta_\kappa \frac{\partial E(t)}{\partial \hat{u}_{ST2ABELC}^k} \frac{\partial \hat{u}_{ST2ABELC}^k}{\partial o_k} \\ &\quad \times \left(\frac{\partial o_k}{\partial o_k^l} \frac{\partial o_k^l}{\partial \underline{\delta}_{ij}} \frac{\partial \underline{\delta}_{ij}}{\partial \kappa_{ik}} + \frac{\partial o_k}{\partial o_k^r} \frac{\partial o_k^r}{\partial \overline{\delta}_{ij}} \frac{\partial \overline{\delta}_{ij}}{\partial \kappa_{ik}} \right) \\ &= \kappa_{ik}(t) + \eta_\kappa \frac{1}{2} e_k(t) \\ &\quad \times \left(\frac{\underline{\upsilon}_{ijk} - o_k^l}{\sum_{j=1}^{n_j} \sum_{i=1}^{n_i} \underline{\delta}_{ij}} \left(\frac{I_i - \kappa_{ik}}{\left(\underline{\tau}_{ij}\right)^2} \right) + \frac{\overline{\upsilon}_{ijk} - o_k^r}{\sum_{j=1}^{n_j} \sum_{i=1}^{n_i} \overline{\delta}_{ij}} \right. \\ &\quad \left. \times \left(\frac{I_i - \kappa_{ik}}{\left(\overline{\tau}_{ij}\right)^2} \right) \right) \end{aligned} \tag{35}$$

$$\begin{aligned}\underline{\tau}_{ij}(t+1) &= \underline{\tau}_{ij}(t) - \eta_\tau \frac{\partial E(t)}{\partial \underline{\tau}_{ij}} \\ &= \underline{\tau}_{ij}(t) - \eta_\tau \frac{\partial E(t)}{\partial \hat{u}_{ST2ABELC}^k} \frac{\partial \hat{u}_{ST2ABELC}^k}{\partial o_k} \frac{\partial o_k}{\partial o_k^l} \frac{\partial o_k^l}{\partial \underline{\delta}_{ij}} \\ &\quad \times \frac{\partial \underline{\delta}_{ij}}{\partial \underline{\tau}_{ij}} \\ &= \underline{\tau}_{ij}(t) + \eta_\tau \frac{1}{2} e_k(t) \frac{\underline{\upsilon}_{ijk} - o_k^l}{\sum_{j=1}^{n_j} \sum_{i=1}^{n_i} \underline{\delta}_{ij}} \left(\frac{(I_i - \kappa_{ik})^2}{\left(\underline{\tau}_{ij}\right)^3} \right) \end{aligned} \tag{36}$$

$$\begin{aligned}\overline{\tau}_{ij}(t+1) &= \overline{\tau}_{ij}(t) - \eta_\tau \frac{\partial E(t)}{\partial \overline{\tau}_{ij}} \\ &= \overline{\tau}_{ij}(t) - \eta_\tau \frac{\partial E(t)}{\partial \hat{u}_{ST2ABELC}^k} \frac{\partial \hat{u}_{ST2ABELC}^k}{\partial o_k} \frac{\partial o_k}{\partial o_k^r} \frac{\partial o_k^r}{\partial \overline{\delta}_{ij}} \\ &\quad \times \frac{\partial \overline{\delta}_{ij}}{\partial \overline{\tau}_{ij}} \\ &= \overline{\tau}_{ij}(t) + \eta_\tau \frac{1}{2} e_k(t) \frac{\overline{\upsilon}_{ijk} - o_k^r}{\sum_{j=1}^{n_j} \sum_{i=1}^{n_i} \overline{\delta}_{ij}} \left(\frac{(I_i - \kappa_{ik})^2}{\left(\overline{\tau}_{ij}\right)^3} \right) \end{aligned} \tag{37}$$

where η_υ, η_κ, η_τ are the positive learning-rates.

D. THE SELF-ORGANIZING ALGORITHMS

The proposed controller ST2ABELC is set up with a number of fuzzy rules based on initial initialization. However, having too many rules will bring a computational burden, even making the system ineffective. On the contrary, too few fuzzy rules will not cover the changes in the input, leading to poor performance. To solve this problem, an effective self-organization mechanism is built to simplify the task of structuring fuzzy rules flexibly. The proposed self-organization mechanism aims to expand or prune the membership functions and fuzzy rules as needed to achieve a reasonably optimal structure.

The conditions for expanding new rules are based on the maximum membership grades, $\varphi^i_{\max}$, and the gernerating threshold, φ_e, as follow:

$$\varphi^i_{\max} < \varphi_e \tag{38}$$

where $\varphi^i_{\max} = max\left[\varphi_{i11}, \ldots, \varphi_{i1n_k}, \varphi_{i21}, \ldots, \varphi_{i2n_k}, \ldots, \varphi_{in_j1}, \ldots, \varphi_{in_jn_k}\right]$ and $\varphi_{ijk} = \frac{\underline{\varphi}_{ijk} + \overline{\varphi}_{ijk}}{2}$

The expression defining the new asymmetric type-2 Gaussian membership function is as follows:

$$\left[\overline{c}^l_{ij}, \underline{c}^l_{ij}, \underline{c}^r_{ij}, \overline{c}^r_{ij}\right] = [I_i(t) - \Delta c, I_i(t) - \Delta c/2, I_i(t) + \Delta c/2, I_i(t) + \Delta c] \tag{39}$$

$$\left[\underline{v}^l_{ij}, \overline{v}^l_{ij}, \underline{v}^r_{ij}, \overline{v}^r_{ij}\right] = [v_{init} - \Delta v, v_{init} - \Delta v/2, v_{init} + \Delta v/2, v_{init} + \Delta v] \tag{40}$$

where Δc and Δv respectively are the uncertain value for the mean and variance of the GMFs; v_{init} is the initial value for the variance of the GMFs.

The conditions for pruning unused rules are based on the minimum membership grades, $\varphi^i_{\min}$, and the pruning threshold, φ_p, as follows:

$$\varphi^i_{\min} < \varphi_p \tag{41}$$

where $\varphi^i_{\min} = min\left[\varphi_{i11}, \ldots, \varphi_{i1n_k}, \varphi_{i21}, \ldots, \varphi_{i2n_k}, \ldots, \varphi_{in_j1}, \ldots, \varphi_{in_jn_k}\right]$

E. SIMULATION STUDIES

This section presents our study on using the proposed ST2ABELC controller for simultaneous synchronization of chaotic satellite systems in two examples: with and without considering disturbances and external noise. The initial condition is optioned as $\boldsymbol{a}(t) = [5,\ 3,\ 4]$, $\boldsymbol{b}(t) = [2,\ -2,\ 1]$, $T_1 = 3$, $T_2 = 2$, $T_3 = 1$, $\boldsymbol{\varepsilon}(t) = [\cos \pi t, 0.5 \cos t, 1.5 \cos 2t]$ and $\Delta \boldsymbol{f}(b) = 0.8\,[b_1(t), b_2(t), b_3(t)]$. For the self-organizing mechanism of ST2ABELC, the generating and pruning thresholds are chosen as $\varphi_e = 0.15$, $\varphi_p = 0.01$, $\Delta c = 0.1$, $\Delta v = 0.05$ and $v_{init} = 0.1$.

Case 1: The results of synchronizing chaotic satellite systems without considering disturbances and external noise are presented in Figs. 4-8. The trajectories of the synchronization process in two and three dimensions, using the proposed ST2ABELC controller, are depicted in Fig. 4. The trajectories of the synchronization process in the time domain are shown in Fig. 5. The synchronization control signals and trajectory tracking errors are respectively given in Figs. 6 and 7. The adjustments of the membership function using self-organizing algorithms are shown in Fig. 8. From these simulation result figures, the proposed ST2ABELC controller can rapidly synchronize satellite systems, with the tracking error converging to zero quickly.

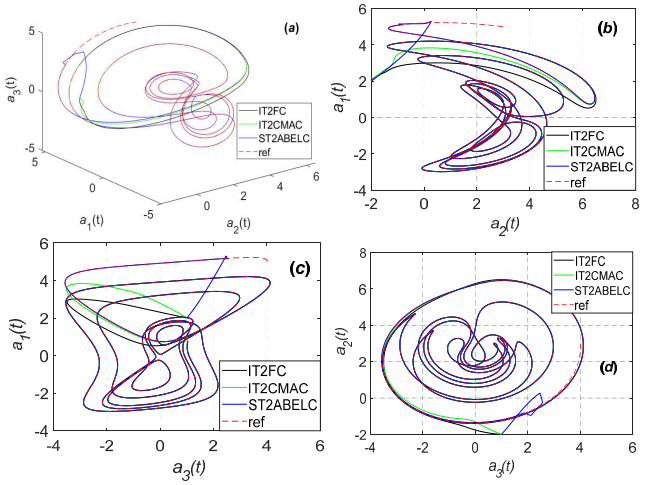

FIGURE 4. The trajectories of the synchronization process for Case 1. (a) Depicted on the 3-D plane; (b) Depicted on a_1 b_1 - a_2 b_2 plane; (c) Depicted on a_1 b_1 - a_3 b_3 plane; (d) Depicted on a_2 b_2 - a_3 b_3 plane.

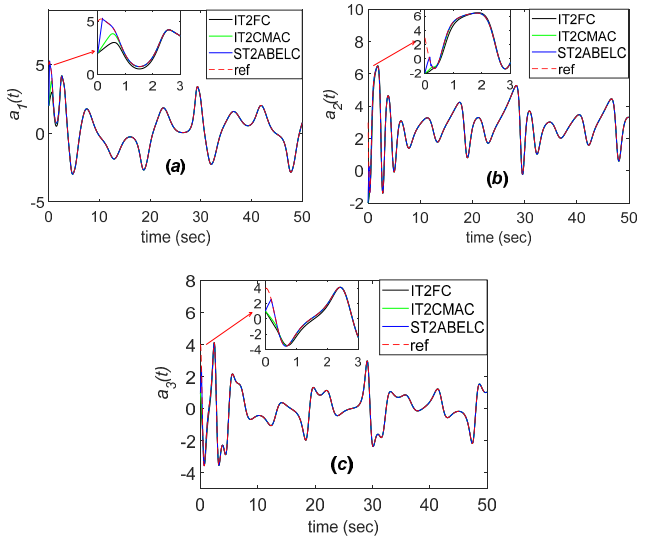

FIGURE 5. The trajectories of the synchronization process in the time domain for Case 1.

In Case 2, we consider the synchronization of chaotic satellite systems in the presence of disturbances and external noise. The results are presented in Figs. 9-13. Fig. 9 depicts the trajectories of the synchronization process in two and three dimensions using the proposed ST2ABELC controller. Fig. 10 showcases the trajectories of the synchronization

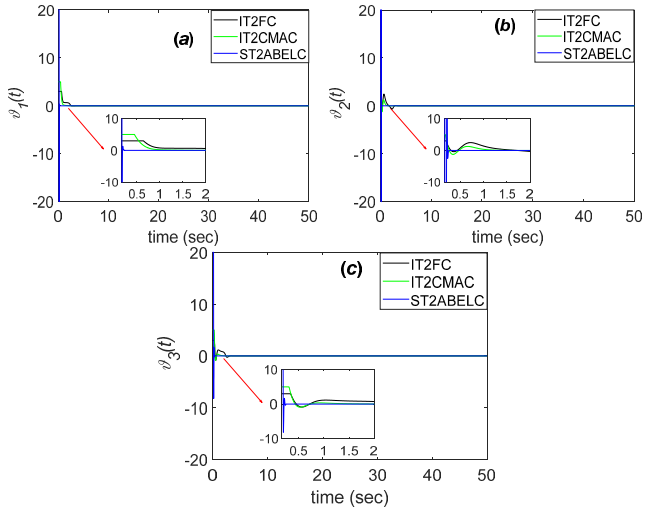

FIGURE 6. The synchronization control signals for Case 1.

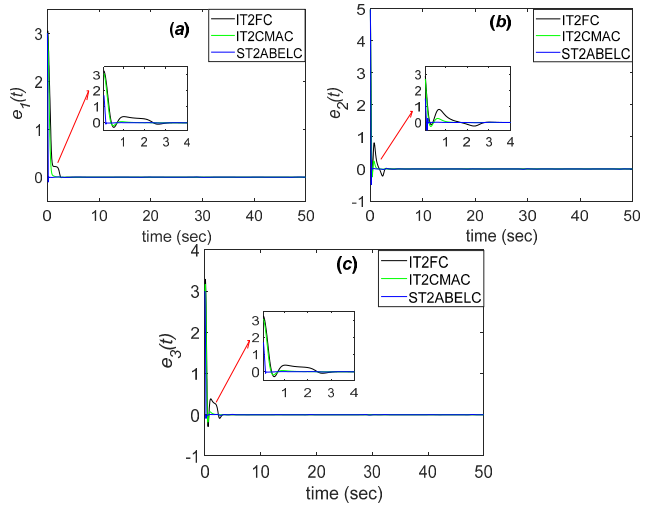

FIGURE 7. The trajectory tracking errors for Case 1.

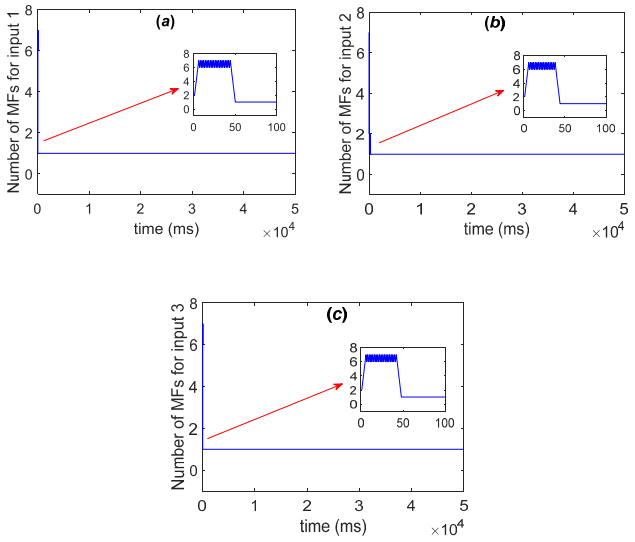

FIGURE 8. The adjustments of the membership function using self-organizing algorithms for Case 1.

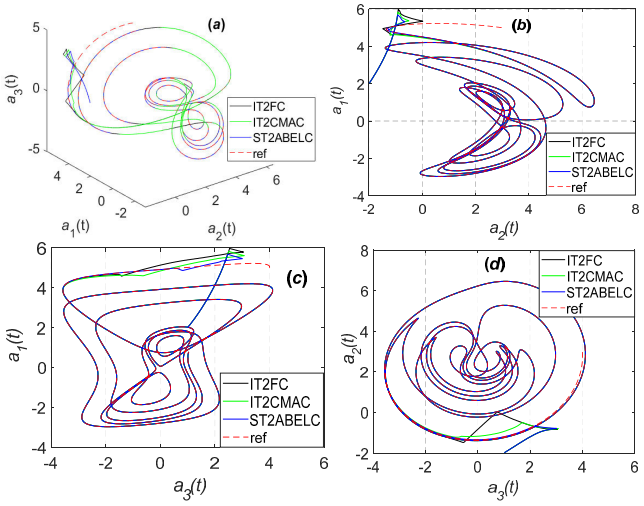

FIGURE 9. The trajectories of the synchronization process for Case 2. (a) Depicted on the 3-D plane; (b) Depicted on a_1 b_1 - a_2 b_2 plane; (c) Depicted on a_1 b_1 - a_3 b_3 plane; (d) Depicted on a_2 b_2 - a_3 b_3 plane.

process in the time domain. Additionally, Figs. 11 and 12 provide information on synchronization signals and trajectory tracking errors, respectively. Finally, Fig. 13 illustrates the adjustments of the membership function achieved through self-organizing algorithms. From the simulation results depicted in the figures for this case, it is evident that the ST2ABELC controller proposed in this scenario can rapidly achieve synchronization for satellite systems, with the tracking error swiftly converging to zero even in the presence of disturbances and external noise.

In both cases, the proposed ST2ABELC controller demonstrated its capability to rapidly achieve synchronization. The root mean square error (RMSE) comparison between the proposed control system and alternative advanced methods is detailed in Table 3. Notably, the ST2ABELC controller demonstrates superior synchronization performance when contrasted with both the interval type-2 fuzzy controller (IT2FC) and the interval type-2 cerebellar model articulation controller (IT2CMAC). In the first scenario, where disturbances and external noise were not considered, the synchronization process was depicted in Figs. 4-8, with the tracking error converging to zero quickly. This showcases the controller's effectiveness in ideal conditions. In the second scenario, where disturbances and external noise were present, the controller's performance remained impressive. Figs. 9-13 provide a detailed view of the synchronization process, highlighting the controller's ability to handle challenging real-world conditions. Even in the presence of disturbances and external noise, the tracking error swiftly converged to zero. These results underscore the robustness and efficiency of the proposed ST2ABELC controller in achieving synchronization for satellite systems, making it a

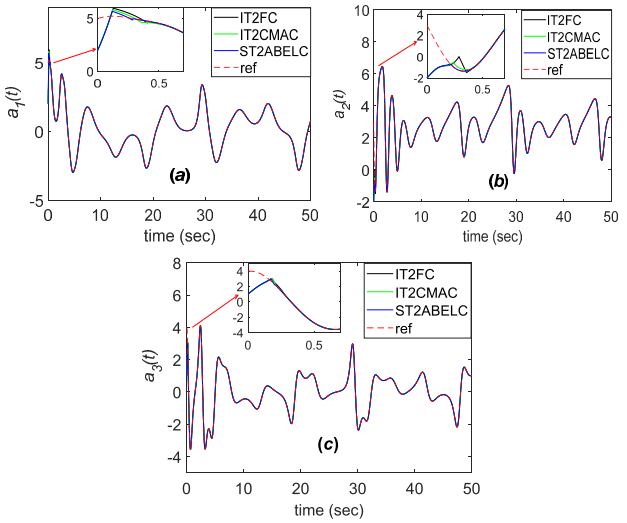

FIGURE 10. The trajectories of the synchronization process in the time domain for Case 2.

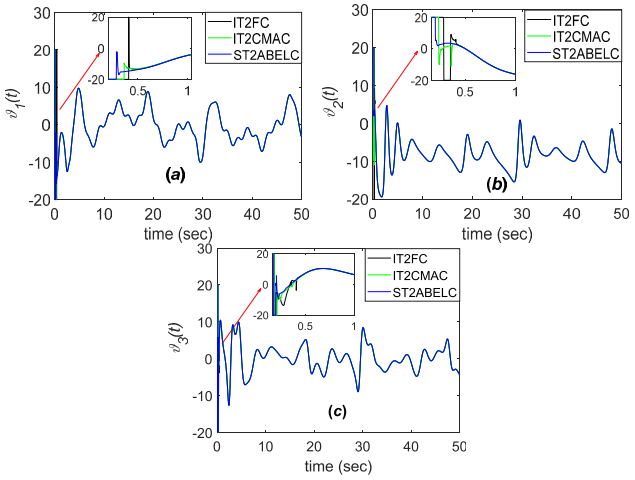

FIGURE 11. The synchronization control signals for Case 2.

promising choice for real-world applications where disturbances and external factors cannot be ignored.

TABLE 3. The RMSE comparison results.

	Computation time (s)	Case 1	Case 2
IT2FC	0.0152	0.4205	0.6170
IT2CMAC	0.0165	0.3831	0.4203
ST2ABELC	0.0217	0.3598	0.3786

The selection of parameters for our proposed synchronizer significantly affects the system's performance. For instance, when determining the generating threshold, opting for a large value results in the creation of extensive membership functions, thereby demanding high computation time. Conversely, selecting a small value makes it challenging to add new

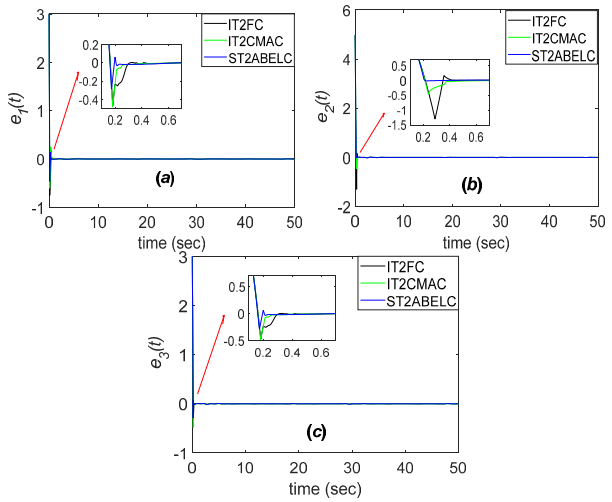

FIGURE 12. The trajectory tracking errors for Case 2.

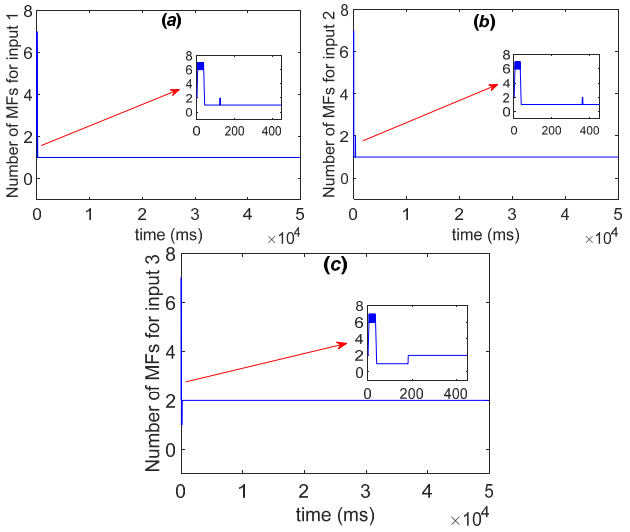

FIGURE 13. The adjustments of the membership function using self-organizing algorithms for Case 2.

membership functions. Similarly, the choice of a pruning threshold holds importance; a large value may delete all membership functions, while a small value may make it difficult to remove unused membership functions. In this study, we employ a trial-and-error approach to determine these thresholds. In forthcoming endeavors, our attention will be directed towards the utilization of novel methodologies to enhance the optimization of these parameters. Additionally, our forthcoming research endeavors will be dedicated to the application of the proposed methodology within targeted practical domains. Prospective applications of synchronizing chaotic satellite systems encompass but are not limited to: chaotic communication, rendezvous and docking control of satellites, and image encryption.

IV. CONCLUSION

This paper has introduced a pioneering approach for the integration of synchronization techniques into chaotic satellite

systems utilizing Type-2 Fuzzy Brain Emotional Learning Control and Asymmetric Membership Function. The presented methodology has been devised with the primary goal of enhancing the cognitive control capabilities of satellite systems, thereby ensuring heightened adaptability and superior performance in dynamic and uncertain environments. The Type-2 Fuzzy BELC system, bolstered by emotional learning mechanisms, equips satellite systems with the capability to make intelligent decisions and adapt their control strategies based on prior experiences. When coupled with AMF, this control system adeptly manages uncertainties and imprecisions in the system's inputs, further reinforcing its reliability. Moreover, the incorporation of self-organizing algorithms facilitates the automatic organization and adaptation of the control network, thereby ensuring optimal system performance and scalability. Through extensive simulations carried out in representative chaotic satellite system scenarios, this research has unequivocally demonstrated the supremacy of the proposed method.

APPENDIX
PROOF OF CONVERGENCE

Defining:

$$V(t) = \frac{1}{2}(e_k(t))^2 \tag{A1}$$

Then,

$$\begin{aligned}\Delta V(t) &= V(t+1) - V(t) = \frac{1}{2}\left[(e_k(t+1))^2 - (e_k(t))^2\right] \\ &= \Delta e_k(t)\left[\frac{1}{2}\Delta e_k(t) + e_k(t)\right]\end{aligned} \tag{A2}$$

By employing the Taylor expansion linearization approach, the nonlinear function can be transformed into a partially linear form [A1]. As a result

$$e_k(t+1) = e_k(t) + \Delta e_k(t) \cong e_k(t) + \left[\frac{\partial e_k(t)}{\partial \xi}\right]^T \Delta\xi \tag{A3}$$

In this context, ξ representing $\overline{\theta}_{jk}$, $\underline{\theta}_{jk}$, $\underline{c}^l_{ij}$, $\underline{c}^r_{ij}$, $\underline{v}^l_{ij}$, $\underline{v}^r_{ij}$, $\overline{c}^l_{ij}$, $\overline{c}^r_{ij}$, $\overline{v}^l_{ij}$, $\overline{v}^r_{ij}$, $\overline{\upsilon}_{ijk}$, $\underline{\upsilon}_{ijk}$, κ_{ik}, $\underline{\tau}_{ij}$, and $\overline{\tau}_{ij}$.

From (23)-(37), obtain

$$\begin{aligned}\Delta\xi &= -\eta_\xi \frac{\partial E(t)}{\partial \xi} \\ &= -\eta_\xi \frac{\partial E(t)}{\partial e_k(t)} \frac{\partial e_k(t)}{\partial k(t)} \frac{\partial k(t)}{\partial u^k_{ST2ABELC}} \frac{\partial u^k_{ST2ABELC}}{\partial \xi} \\ &= \eta_\xi e_k(t) \Xi_\xi(t)\end{aligned} \tag{A4}$$

In (A4), the term $\Xi_\xi(t) = \frac{\partial u^k_{ST2ABELC}}{\partial \xi}$ can be given as

$$\begin{aligned}\boldsymbol{\Xi}_\xi(t) &= \frac{\partial u^k_{ST2ABELC}}{\partial \underline{\boldsymbol{\theta}}} \\ &= \left[\frac{\partial u^k_{ST2ABELC}}{\partial \underline{\theta}_{11}}, \ldots, \frac{\partial u^k_{ST2ABELC}}{\partial \underline{\theta}_{1n_k}}, \ldots, \right. \\ &\quad \left. \frac{\partial u^k_{ST2ABELC}}{\partial \underline{\theta}_{n_j1}}, \ldots, \frac{\partial u^k_{ST2ABELC}}{\partial \underline{\theta}_{n_jn_k}}\right]^T\end{aligned} \tag{A5}$$

$$\begin{aligned}\boldsymbol{\Xi}_\xi(t) &= \frac{\partial u^k_{ST2ABELC}}{\partial \overline{\boldsymbol{\theta}}} \\ &= \left[\frac{\partial u^k_{ST2ABELC}}{\partial \overline{\theta}_{11}}, \ldots, \frac{\partial u^k_{ST2ABELC}}{\partial \overline{\theta}_{1n_k}}, \ldots, \right. \\ &\quad \left. \frac{\partial u^k_{ST2ABELC}}{\partial \overline{\theta}_{n_j1}}, \ldots, \frac{\partial u^k_{ST2ABELC}}{\partial \overline{\theta}_{n_jn_k}}\right]^T\end{aligned} \tag{A6}$$

$$\begin{aligned}\boldsymbol{\Xi}_\xi(t) &= \frac{\partial u^k_{ST2ABELC}}{\partial \underline{\boldsymbol{c}}^l} \\ &= \left[\frac{\partial u^k_{ST2ABELC}}{\partial \underline{c}^l_{11}}, \ldots, \frac{\partial u^k_{ST2ABELC}}{\partial \underline{c}^l_{1n_k}}, \ldots, \right. \\ &\quad \left. \frac{\partial u^k_{ST2ABELC}}{\partial \underline{c}^l_{n_j1}}, \ldots, \frac{\partial u^k_{ST2ABELC}}{\partial \underline{c}^l_{n_jn_k}}\right]^T\end{aligned} \tag{A7}$$

$$\begin{aligned}\boldsymbol{\Xi}_\xi(t) &= \frac{\partial u^k_{ST2ABELC}}{\partial \underline{\boldsymbol{c}}^r} \\ &= \left[\frac{\partial u^k_{ST2ABELC}}{\partial \underline{c}^r_{11}}, \ldots, \frac{\partial u^k_{ST2ABELC}}{\partial \underline{c}^r_{1n_k}}, \ldots, \right. \\ &\quad \left. \frac{\partial u^k_{ST2ABELC}}{\partial \underline{c}^r_{n_j1}}, \ldots, \frac{\partial u^k_{ST2ABELC}}{\partial \underline{c}^r_{n_jn_k}}\right]^T\end{aligned} \tag{A8}$$

$$\begin{aligned}\boldsymbol{\Xi}_\xi(t) &= \frac{\partial u^k_{ST2ABELC}}{\partial \underline{\boldsymbol{v}}^l} \\ &= \left[\frac{\partial u^k_{ST2ABELC}}{\partial \underline{v}^l_{11}}, \ldots, \frac{\partial u^k_{ST2ABELC}}{\partial \underline{v}^l_{1n_k}}, \ldots, \right. \\ &\quad \left. \frac{\partial u^k_{ST2ABELC}}{\partial \underline{v}^l_{n_j1}}, \ldots, \frac{\partial u^k_{ST2ABELC}}{\partial \underline{v}^l_{n_jn_k}}\right]^T\end{aligned} \tag{A9}$$

$$\begin{aligned}\boldsymbol{\Xi}_\xi(t) &= \frac{\partial u^k_{ST2ABELC}}{\partial \underline{\boldsymbol{v}}^r} \\ &= \left[\frac{\partial u^k_{ST2ABELC}}{\partial \underline{v}^r_{11}}, \ldots, \frac{\partial u^k_{ST2ABELC}}{\partial \underline{v}^r_{1n_k}}, \ldots, \right. \\ &\quad \left. \frac{\partial u^k_{ST2ABELC}}{\partial \underline{v}^r_{n_j1}}, \ldots, \frac{\partial u^k_{ST2ABELC}}{\partial \underline{v}^r_{n_jn_k}}\right]^T\end{aligned} \tag{A10}$$

$$\begin{aligned}\boldsymbol{\Xi}_\xi(t) &= \frac{\partial u^k_{ST2ABELC}}{\partial \overline{\boldsymbol{c}}^l} \\ &= \left[\frac{\partial u^k_{ST2ABELC}}{\partial \overline{c}^l_{11}}, \ldots, \frac{\partial u^k_{ST2ABELC}}{\partial \overline{c}^l_{1n_k}}, \ldots, \right. \\ &\quad \left. \frac{\partial u^k_{ST2ABELC}}{\partial \overline{c}^l_{n_j1}}, \ldots, \frac{\partial u^k_{ST2ABELC}}{\partial \overline{c}^l_{n_jn_k}}\right]^T\end{aligned} \tag{A11}$$

$$\begin{aligned}\boldsymbol{\Xi}_\xi(t) &= \frac{\partial u^k_{ST2ABELC}}{\partial \overline{\boldsymbol{c}}^r} \\ &= \left[\frac{\partial u^k_{ST2ABELC}}{\partial \overline{c}^r_{11}}, \ldots, \frac{\partial u^k_{ST2ABELC}}{\partial \overline{c}^r_{1n_k}}, \ldots, \right.\end{aligned}$$

$$\left.\frac{\partial u^k_{ST2ABELC}}{\partial \overline{c}^r_{n_j 1}}, \ldots, \frac{\partial u^k_{ST2ABELC}}{\partial \overline{c}^r_{n_j n_k}}\right]^T \tag{A12}$$

$$\begin{aligned}\Xi_\xi(t) &= \frac{\partial u^k_{ST2ABELC}}{\partial \overline{\boldsymbol{v}}^l} \\ &= \left[\frac{\partial u^k_{ST2ABELC}}{\partial \overline{v}^l_{11}}, \ldots, \frac{\partial u^k_{ST2ABELC}}{\partial \overline{v}^l_{1n_k}}, \ldots, \right. \\ &\quad \left. \frac{\partial u^k_{ST2ABELC}}{\partial \overline{v}^l_{n_j 1}}, \ldots, \frac{\partial u^k_{ST2ABELC}}{\partial \overline{v}^l_{n_j n_k}}\right]^T \end{aligned} \tag{A13}$$

$$\begin{aligned}\Xi_\xi(t) &= \frac{\partial u^k_{ST2ABELC}}{\partial \overline{\boldsymbol{v}}^r} \\ &= \left[\frac{\partial u^k_{ST2ABELC}}{\partial \overline{v}^r_{11}}, \ldots, \frac{\partial u^k_{ST2ABELC}}{\partial \overline{v}^r_{1n_k}}, \ldots, \right. \\ &\quad \left. \frac{\partial u^k_{ST2ABELC}}{\partial \overline{v}^r_{n_j 1}}, \ldots, \frac{\partial u^k_{ST2ABELC}}{\partial \overline{v}^r_{n_j n_k}}\right]^T \end{aligned} \tag{A14}$$

$$\begin{aligned}\Xi_\xi(t) &= \frac{\partial u^k_{ST2ABELC}}{\partial \underline{\boldsymbol{\upsilon}}} \\ &= \left[\frac{\partial u^k_{ST2ABELC}}{\partial \underline{\upsilon}^r_{i11}}, \ldots, \frac{\partial u^k_{ST2ABELC}}{\partial \underline{\upsilon}^r_{i1n_k}}, \ldots, \right. \\ &\quad \left. \frac{\partial u^k_{ST2ABELC}}{\partial \underline{\upsilon}^r_{in_j 1}}, \ldots, \frac{\partial u^k_{ST2ABELC}}{\partial \underline{\upsilon}^r_{in_j n_k}}\right]^T \end{aligned} \tag{A15}$$

$$\begin{aligned}\Xi_\xi(t) &= \frac{\partial u^k_{ST2ABELC}}{\partial \overline{\boldsymbol{\upsilon}}} \\ &= \left[\frac{\partial u^k_{ST2ABELC}}{\partial \overline{\upsilon}_{i11}}, \ldots, \frac{\partial u^k_{ST2ABELC}}{\partial \overline{\upsilon}_{i1n_k}}, \ldots, \right. \\ &\quad \left. \frac{\partial u^k_{ST2ABELC}}{\partial \overline{\upsilon}_{in_j 1}}, \ldots, \frac{\partial u^k_{ST2ABELC}}{\partial \overline{\upsilon}_{in_j n_k}}\right]^T \end{aligned} \tag{A16}$$

$$\begin{aligned}\Xi_\xi(t) &= \frac{\partial u^k_{ST2ABELC}}{\partial \boldsymbol{\kappa}} \\ &= \left[\frac{\partial u^k_{ST2ABELC}}{\partial \kappa_{11}}, \ldots, \frac{\partial u^k_{ST2ABELC}}{\partial \kappa_{1n_k}}, \ldots, \right. \\ &\quad \left. \frac{\partial u^k_{ST2ABELC}}{\partial \kappa_{n_j 1}}, \ldots, \frac{\partial u^k_{ST2ABELC}}{\partial \kappa_{n_i n_k}}\right]^T \end{aligned} \tag{A17}$$

$$\begin{aligned}\Xi_\xi(t) &= \frac{\partial u^k_{ST2ABELC}}{\partial \underline{\boldsymbol{\tau}}} \\ &= \left[\frac{\partial u^k_{ST2ABELC}}{\partial \underline{\tau}_{11}}, \ldots, \frac{\partial u^k_{ST2ABELC}}{\partial \underline{\tau}_{1n_k}}, \ldots, \right. \\ &\quad \left. \frac{\partial u^k_{ST2ABELC}}{\partial \underline{\tau}_{n_j 1}}, \ldots, \frac{\partial u^k_{ST2ABELC}}{\partial \underline{\tau}_{n_j n_k}}\right]^T \end{aligned} \tag{A18}$$

$$\begin{aligned}\Xi_\xi(t) &= \frac{\partial u^k_{ST2ABELC}}{\partial \overline{\boldsymbol{\tau}}} \\ &= \left[\frac{\partial u^k_{ST2ABELC}}{\partial \overline{\tau}_{11}}, \ldots, \frac{\partial u^k_{ST2ABELC}}{\partial \overline{\tau}_{1n_k}}, \ldots, \right. \\ &\quad \left. \frac{\partial u^k_{ST2ABELC}}{\partial \overline{\tau}_{n_j 1}}, \ldots, \frac{\partial u^k_{ST2ABELC}}{\partial \overline{\tau}_{n_j n_k}}\right]^T \end{aligned} \tag{A19}$$

From (A3), obtain

$$\frac{\partial e_k(t)}{\partial \xi} = \frac{\partial e_k(t)}{\partial u^k_{ST2ABELC}} \frac{\partial u^k_{ST2ABELC}}{\partial \xi} = -\Xi_\xi(t) \tag{A20}$$

Through the use of (A4) and (A20), we can reformulate (A2) as follows:

$$\begin{aligned}\Delta V(t) &= \Delta e_k(t)\left[\frac{1}{2}\Delta e_k(t) + e_k(t)\right] \\ &= \left(\left[\frac{\partial e_k(t)}{\partial \xi}\right]^T \Delta\xi\right)\left[\frac{1}{2}\left(\left[\frac{\partial e_k(t)}{\partial \xi}\right]^T \Delta\xi\right) + e_k(t)\right] \\ &= -\left[\Xi_\xi(t)\right]^T \eta_\xi e_k(t)\Xi_\xi(t)\left[-\frac{1}{2}\left[\Xi_\xi(t)\right]^T\right. \\ &\quad \left.\times \eta_\xi e_k(t)\Xi_\xi(t) + e_k(t)\right] \\ &= \frac{1}{2}\eta_\xi\,(e_k(t))^2 \left\|\Xi_\xi(t)\right\|^2 \left[\eta_\xi \left\|\Xi_\xi(t)\right\|^2 - 2\right] \end{aligned} \tag{A21}$$

From (A21), when η_ξ is deliberately chosen to satisfy $0 < \eta_\xi < \frac{2}{\|\Xi_\xi(t)\|^2}$, it results in a condition where $\Delta V(t) < 0$. Consequently, this choice ensures the stability of the control system presented in this study.

REFERENCES

[1] M. Shafiq, I. Ahmad, O. A. Almatroud, and M. M. Al-Sawalha, "Robust attitude control of the three-dimensional unknown chaotic satellite system," *Trans. Inst. Meas. Control*, vol. 44, no. 7, pp. 1484–1504, Apr. 2022.

[2] A. Azam, M. Aqeel, and D. A. Sunny, "Generation of multidirectional mirror symmetric multiscroll chaotic attractors (MSMCA) in double wing satellite chaotic system," *Chaos, Solitons Fractals*, vol. 155, Feb. 2022, Art. no. 111715.

[3] S. Kumar, A. E. Matouk, H. Chaudhary, and S. Kant, "Control and synchronization of fractional-order chaotic satellite systems using feedback and adaptive control techniques," *Int. J. Adapt. Control Signal Process.*, vol. 35, no. 4, pp. 484–497, Apr. 2021.

[4] M. Shafiq and I. Ahmad, "Synchronization of chaotic satellite systems with an unknown parameter," *J. Vibrat. Control*, 2023, doi: 10.1177/10775463231203276.

[5] S. Hamel, A. Boulkroune, and A. J. C. Bouzeriba, "Function vector synchronization based on fuzzy control for uncertain chaotic systems with dead-zone nonlinearities," *Complexity*, vol. 21, no. S1, pp. 234–249, 2016.

[6] A. Khan and S. Kumar, "T-S fuzzy modeling and predictive control and synchronization of chaotic satellite systems," *Int. J. Model. Simul.*, vol. 39, no. 3, pp. 203–213, Jul. 2019.

[7] A. Boulkroune, S. Hamel, A. T. Azar, and S. Vaidyanathan, "Fuzzy control-based function synchronization of unknown chaotic systems with dead-zone input," in *Advances in Chaos Theory and Intelligent Control* (Studies in Fuzziness and Soft Computing), vol. 337, A. Azar and S. Vaidyanathan, Eds. Cham, Switzerland: Springer, 2016, pp. 699–718, doi: 10.1007/978-3-319-30340-6_29.

[8] O. Silahtar, F. Kutlu, Ö. Atan, and O. Castillo, "Rendezvous and docking control of satellites using chaos synchronization method with intuitionistic fuzzy sliding mode control," in *Fuzzy Logic and Neural Networks for Hybrid Intelligent System Design*. Cham, Switzerland: Springer, 2023, pp. 177–197.

[9] S. Farzami, R. Esmaelzadeh, and M. R. Taheri, "Chaotic satellite synchronization using neural controllers," in *Proc. 7th Int. Conf. Recent Adv. Space Technol. (RAST)*, Jun. 2015, pp. 99–104.

[10] S. F. Sarcheshmeh, R. Esmaelzadeh, and M. Afshari, "Chaotic satellite synchronization using neural and nonlinear controllers," *Chaos, Solitons Fractals*, vol. 97, pp. 19–27, Apr. 2017.

[11] A. Khan and S. Kumar, "Measuring chaos and synchronization of chaotic satellite systems using sliding mode control," *Optim. Control Appl. Methods*, vol. 39, no. 5, pp. 1597–1609, Sep. 2018.
[12] S. M. Hamidzadeh and A. Zarringhalam, "Attitude control of chaotic satellite with unknown input and uncertainties based on sliding control," *Int. J. Comput. Appl.*, vol. 97, no. 3, pp. 32–36, Jul. 2014.
[13] P. Pal, G. G. Jin, S. Bhakta, and V. Mukherjee, "Adaptive chaos synchronization of an attitude control of satellite: A backstepping based sliding mode approach," *Heliyon*, vol. 8, no. 11, Nov. 2022, Art. no. e11730.
[14] C.-M. Lin and C.-C. Chung, "Fuzzy brain emotional learning control system design for nonlinear systems," *Int. J. Fuzzy Syst.*, vol. 17, no. 2, pp. 117–128, Jun. 2015.
[15] C.-M. Lin and P. K. Muthusamy, "Intelligent brain emotional learning control system design for nonlinear systems," in *Proc. 11th Asian Control Conf. (ASCC)*, Dec. 2017, pp. 958–963.
[16] P. K. Muthusamy, M. Garratt, H. Pota, J. Wang, and J. M. Kok, "Bidirectional fuzzy brain emotional learning control for aerial robots," in *Proc. IEEE Symp. Ser. Comput. Intell. (SSCI)*, Nov. 2018, pp. 146–153.
[17] J. Zhang, F. Chao, H. Zeng, C.-M. Lin, and L. Yang, "A recurrent wavelet-based brain emotional learning network controller for nonlinear systems," *Soft Comput.*, vol. 26, no. 6, pp. 3013–3028, Mar. 2022.
[18] Q. Zhou, F. Chao, and C.-M. Lin, "A functional-link-based fuzzy brain emotional learning network for breast tumor classification and chaotic system synchronization," *Int. J. Fuzzy Syst.*, vol. 20, no. 2, pp. 349–365, Feb. 2018.
[19] J. LeDoux, "Emotion and the limbic system concept," *Concepts Neurosci.*, vol. 2, pp. 169–199, 1991. [Online]. Available: https://nyuscholars.nyu.edu/en/publications/emotion-and-the-limbic-system-concept
[20] S. Murugan, T.-L. Le, and P. N. Quan, "Adaptive noise cancellation using Petri fuzzy brain emotional learning-based neural network," in *Proc. 6th Int. Conf. Green Technol. Sustain. Develop. (GTSD)*, Jul. 2022, pp. 537–542.
[21] C.-M. Lin and H.-Y. Li, "Adaptive dynamic sliding-mode fuzzy CMAC for voice coil motor using asymmetric Gaussian membership function," *IEEE Trans. Ind. Electron.*, vol. 61, no. 10, pp. 5662–5671, Oct. 2014.
[22] H.-Y. Pan, C.-H. Lee, F.-K. Chang, and S.-K. Chang, "Construction of asymmetric type-2 fuzzy membership functions and application in time series prediction," in *Proc. Int. Conf. Mach. Learn. Cybern.*, Aug. 2007, pp. 2024–2030.
[23] T. Zhao, P. Li, and J. Cao, "Self-organising interval type-2 fuzzy neural network with asymmetric membership functions and its application," *Soft Comput.*, vol. 23, no. 16, pp. 7215–7228, Aug. 2019.
[24] P. Verma, R. Garg, and P. Mahajan, "Asymmetrical interval type-2 fuzzy logic control based MPPT tuning for PV system under partial shading condition," *ISA Trans.*, vol. 100, pp. 251–263, May 2020.
[25] F.-J. Lin, C.-I. Chen, G.-D. Xiao, and P.-R. Chen, "Voltage stabilization control for microgrid with asymmetric membership function-based wavelet Petri fuzzy neural network," *IEEE Trans. Smart Grid*, vol. 12, no. 5, pp. 3731–3741, Sep. 2021.
[26] P. Xu, B. Liu, X. Hu, T. Ouyang, and N. Chen, "State-of-charge estimation for lithium-ion batteries based on fuzzy information granulation and asymmetric Gaussian membership function," *IEEE Trans. Ind. Electron.*, vol. 69, no. 7, pp. 6635–6644, Jul. 2022.
[27] F.-J. Lin, P.-L. Wang, and I.-M. Hsu, "Intelligent nonsingular terminal sliding mode controlled nonlinear time-varying system using RPPFNN-AMF," *IEEE Trans. Fuzzy Syst.*, vol. 32, no. 3, pp. 1036–1049, Mar. 2024.
[28] O. Castillo, R. Martínez-Marroquín, P. Melin, F. Valdez, and J. Soria, "Comparative study of bio-inspired algorithms applied to the optimization of type-1 and type-2 fuzzy controllers for an autonomous mobile robot," *Inf. Sci.*, vol. 192, pp. 19–38, Jun. 2012.
[29] M. M. Zirkohi and T.-C. Lin, "Interval type-2 fuzzy-neural network indirect adaptive sliding mode control for an active suspension system," *Nonlinear Dyn.*, vol. 79, no. 1, pp. 513–526, Jan. 2015.
[30] A. M. El-Nagar, M. El-Bardini, and A. A. Khater, "A class of general type-2 fuzzy controller based on adaptive alpha-plane for nonlinear systems," *Appl. Soft Comput.*, vol. 133, Jan. 2023, Art. no. 109938.
[31] S. B. Pandu, C. K. Sundarabalan, N. S. Srinath, T. S. Krishnan, G. S. Priya, C. Balasundar, J. Sharma, G. Soundarya, P. Siano, and H. H. Alhelou, "Power quality enhancement in sensitive local distribution grid using interval type-II fuzzy logic controlled DSTATCOM," *IEEE Access*, vol. 9, pp. 59888–59899, 2021.
[32] D. Sadaoui, A. Boukabou, N. Merabtine, and M. Benslama, "Predictive synchronization of chaotic satellites systems," *Expert Syst. Appl.*, vol. 38, no. 7, pp. 9041–9045, Jul. 2011.
[33] A. Khan and S. Kumar, "Measure of chaos and adaptive synchronization of chaotic satellite systems," *Int. J. Dyn. Control*, vol. 7, no. 2, pp. 536–546, Jun. 2019.
[34] J. M. V. Grzybowski, M. Rafikov, and E. E. N. Macau, "Chaotic communication on a satellite formation flying—The synchronization issue in a scenario with transmission delays," *Acta Astronautica*, vol. 66, nos. 7–8, pp. 1160–1168, Apr. 2010.
[35] F. W. Alsaade, Q. Yao, S. Bekiros, M. S. Al-Zahrani, A. S. Alzahrani, and H. Jahanshahi, "Chaotic attitude synchronization and anti-synchronization of master-slave satellites using a robust fixed-time adaptive controller," *Chaos, Solitons Fractals*, vol. 165, Dec. 2022, Art. no. 112883.